Model of vibrations as periodically non-stationary random processes for identification of the condition of electrical motor

Roman Yuzefovych[a,b,*,†], Ihor Javorskyj[a,c,†], Oleh Lychak[a,†], Pavlo Semenov[d,†], Roman Khmil[b,†]

[a]*Karpenko Physico-mechanical institute of NAS of Ukraine, 5 Naukova Str., Lviv, 79060, Ukraine*
[b]*Lviv Polytechnic National University, 12 Bandera Str., Lviv, 79013, Ukraine*
[c]*Bydgoszcz University of Sciences and Technology, 7 Al. prof. S. Kaliskiego, Bydgoszcz, 85796, Poland*
[d]*Odessa National Maritime University, 65029, 34 Mechnikova Str., Odessa, Ukraine*

Abstract

Quasi least square (LS) technique was used to identify first- and second-order hidden periodicities in vibration signal. It was shown, that the low-frequency vibration component (< 2 kHz) is adequately described by the periodically non-stationary random processes (PNRP) model. The amplitude spectra of the deterministic oscillations and the time changes in the power of the stochastic part are analyzed. The value of an indicator based on the mean function harmonic power is decisive for detecting failures and monitoring the motor condition. The structures of the PNRP moment functions and the high values of the condition indicator enable us to deduce that motor is in a critical state.

Keywords

electric motor vibration; periodically non-stationary random process; mean and covariance function; basic frequency estimators; condition indicators.

1. Introduction

To calculate the mean, covariance function and their Fourier coefficients using experimental data, we need to apply methods of statistical analysis of PNRP, such as coherent (synchronous) averaging [1−10], or the component [11] or the least squares [12] methods. The suitability of a given technique depends on the specifics of the experimental data, the purpose of the analysis, and the required accuracy, but all these methods can be used in cases where the non-stationarity period (basic frequency) is known. In vibration analysis, this period can be in many cases calculated based on technical parameters of investigated mechanism. However, the period values obtained in this way are not sufficiently accurate, and may also vary under real-world conditions. Hence, to ensure that the PNRP analysis is effective, we need to determine the period based on the selected vibration realizations.

2. Methods for determining of the first and second order non-stationarity periods

To determine the non-stationarity period, special functionals can be used [9−16] that are similar to coherent or component statistics, except that a test period is inserted to replace the true period. These functionals have extreme values at points that are asymptotically unbiased and consistent period estimators. The biases of these estimators are on the order $O(T^{-2})$, and the variances are on the order $O(T^{-3})$, where T is the realization length. To improve the efficiency of estimating the

basic frequency, the LS method was proposed in [12]. As the realization length increases, the LS functional for determining the basic frequency of the mean function quickly tends to

$$\hat{F}_1(f)=\frac{1}{2}\sum_{k=1}^{L_1}\left[\left[\hat{m}_k^c(f)\right]^2+\left[\hat{m}_k^s(f)\right]^2\right]\tag{1}$$

where

$$\begin{Bmatrix}\hat{m}_k^c(f)\\\hat{m}_k^s(f)\end{Bmatrix}=\frac{2}{2K+1}\sum_{n=-K}^{K}\xi(nh)\begin{Bmatrix}\cos2k\pi fnh\\\sin2k\pi fnh\end{Bmatrix}\tag{2}$$

and $2T$ is the realization length, $h=\dfrac{T}{k}$ is the sampling step, and L_1 is the number of harmonics. The maximum point $\hat{f}_0$ of (1) is asymptotically unbiased and consistent estimator of the mean basic frequency [12]. The functional at the maximum point $f=\hat{f}_0$ is close to the sum of the time-averaged power of the chosen harmonics:

$$\hat{F}_1\left(\hat{f}_0\right)=\hat{P}_t^{(d)}=\frac{1}{2}\sum_{k=1}^{L_1}\left[\left[\hat{m}_k^c\left(\hat{f}_0\right)\right]^2+\left[\hat{m}_k^s\left(\hat{f}_0\right)\right]^2\right]$$

The quantities $\hat{m}_k^s(\hat{f}_0)$ and $\hat{m}_k^c(\hat{f}_0)$ are asymptotically unbiased and consistent estimators of the Fourier coefficients for the mean function [17-19]. Hence, based on the statistical expression

$$\hat{m}_0=\frac{1}{2K+1}\sum_{n=-K}^{K}\xi(nh)$$

we can form the mean function estimator

$$\hat{m}\left(t,\hat{f}_0\right)=\hat{m}_0+\sum_{k=1}^{L}\left[\hat{m}_k^c\left(\hat{f}_0\right)\cos2k\pi\hat{f}_0t+\hat{m}_k^s\left(\hat{f}_0\right)\sin2k\pi\hat{f}_0t\right]\tag{3}$$

The expression in (3) is the interpolation formula for the mean function for all $t\in\left[0;f_0^{-1}\right]$ if the condition

$$h\le\frac{1}{\hat{f}_0\left(4L_1+1\right)},$$

is satisfied [11]. The function in (2) describes the deterministic oscillations. Their amplitudes and phase spectra are defined by the expressions:

$$\hat{A}\left(k\hat{f}_0\right)=\left[\left[\hat{m}_k^c\left(\hat{f}_0\right)\right]^2+\left[\hat{m}_k^s\left(\hat{f}_0\right)\right]^2\right]^{\frac{1}{2}},\quad\varphi_k\left(k\hat{f}_0\right)=\text{arctg}\frac{\hat{m}_k^s\left(\hat{f}_0\right)}{\hat{m}_k^c\left(\hat{f}_0\right)}\tag{4}$$

As a summary of the foregoing discussion, we present step-by-step procedures for determining the deterministic part of the vibration as follows:

- Using the experimental time series $\xi(nh)$, we form the statistics in (2);
- By substituting into (1) the formulae in (2) we can form the functional for the numerical analysis. The number L_1 is chosen to be close to the ratio f_m/f_r, where f_m is the signal spectrum high boundary frequency and f_r is the rotation frequency;

- We then calculate the functional in (1) for the frequencies belonging to the interval $[f_1, f_2]$, which contain the rotation frequency f_r. If we want to find the basic frequency to an accuracy of 10^{-3} Hz, we choose a calculation step of $\Delta f = 10^{-3}$ Hz;
- The maximum points of (10) are taken as the estimator of the mean basic frequency $\hat{f}_0$, and the value $F(\hat{f}_0)$ is accepted as the estimator of power for deterministic oscillations;
- By substituting $f = \hat{f}_0$ into (11), we calculate the mean Fourier coefficients, and the amplitude and phase spectra;
- Using the interpolation formula in (3), we calculate the mean values for all $t \in [0; \hat{P}]$, where $\hat{P} = 1/\hat{f}$. Assuming that $\hat{m}(t, \hat{f}_0) = m(t + \hat{P}, \hat{f}_0)$, we can separate the stochastic part $\overset{\circ}{\xi}(nh) = \xi(nh) - \hat{m}(nh, \hat{f}_o)$

The LS functional for estimating the variance in the basic frequency for large K can be represented in the form:

$$F_2\left(\hat{f}_0\right) = P_t^{(s)} = \frac{1}{2} \sum_{k=1}^{L_2} \left[\left[\hat{R}_k^c\left(0, \hat{f}_0\right)\right]^2 + \left[\hat{R}_k^s\left(0, \hat{f}_0\right)\right]^2 \right] \qquad (5)$$

where

$$\begin{Bmatrix} \hat{R}_k^c(0,f) \\ \hat{R}_k^s(0,f) \end{Bmatrix} = \frac{2}{2K+1} \sum_{n=-K}^{K} \overset{\circ}{\xi}{}^2(nh) \begin{Bmatrix} \cos 2k\pi f n h \\ \sin 2k\pi f n h \end{Bmatrix}, \qquad (6)$$

and L_2 is the number of harmonics. The maximum point of the expression in (5) is an asymptotically unbiased and consistent estimator of the variance in the basic frequency. By substituting $f = \hat{f}_0$ into (6), we obtain statistics for calculating the Fourier coefficients of the variance. Hence, the quantity

$$\hat{F}_2(f) = \frac{1}{2} \sum_{k=1}^{L_2} \left[\left[\hat{R}_k^c(0,f)\right]^2 + \left[\hat{R}_k^s(0,f)\right]^2 \right],$$

We can obtain the variance estimator for $t \in [0; f_0^{-1}]$ all on the basis of $\hat{R}_k^c(0, \hat{f}_0)$, $\hat{R}_k^s(0, \hat{f}_0)$ and the statistical expression

$$\hat{R}_0(0) = \frac{1}{2K+1} \sum_{n=-K}^{K} \overset{\circ}{\xi}{}^2(nh),$$

using the interpolation formula

$$\hat{R}\left(t, 0, \hat{f}_0\right) = \hat{R}_0(0) + \sum_{k=1}^{L_2} \left[\hat{R}_k^c\left(0, \hat{f}_0\right) \cos 2k\pi \hat{f}_0 t + \hat{R}_k^s\left(0, \hat{f}_0\right) \sin 2k\pi \hat{f}_0 t \right] \qquad (7)$$

Aliasing errors are absent if the inequality

$$h \le \frac{1}{\hat{f}_0(4L_2 + 1)}$$

is fulfilled [11]. The function in (7) describes the shape of the periodic time changes in the power of the stochastic part. To characterize these changes, it is advisable to calculate the amplitude and phase spectra as follows:

$$\hat{V}\left(k\hat{f_0}\right)=\left[\left[\hat{R}_k^c\left(0,\hat{f_0}\right)\right]^2+\left[\hat{R}_k^s\left(0,\hat{f_0}\right)\right]^2\right]^{\frac{1}{2}}, \quad \psi_k=\text{arctg}\frac{\hat{R}_k^s\left(0,\hat{f_0}\right)}{\hat{R}_k^c\left(0,\hat{f_0}\right)} \tag{8}$$

It follows from the above that the procedures used for estimating the vibration variance are similar to those for estimating the mean. In the present case, only the squared centered realization is processed, and the functional in (5) is calculated. Since the variance in the time changes is the result of correlations of the harmonic belonging to the signal spectrum and shifted by kf_0, where k is number of the variance harmonic, then the integer number L_2 is limited by the ratio of the signal bandwidth to the rotation frequency.

The mean and variance spectra are used to define the health status of the mechanism. The condition indicators can also be formed on the basis of a harmonic composition. The first indicator is determined by the ratio of the sum of the time-averaged powers of the harmonics for deterministic oscillations to the time-averaged power of the stochastic component

$$I_1=\frac{1}{2}\sum_{k=1}^{L_1}\hat{A}_k^2\left(k\hat{f_0}\right)\Big/\hat{R}_0(0)$$

The second indicator is a measure of the signal non-stationarity of the second order. It is defined as the ratio of the sum of amplitudes of the variance harmonics to its time-averaged value, . $\quad I_2=\frac{1}{2}\sum_{k=1}^{L_2}\hat{V}\left(k\hat{f_0}\right)\Big/\hat{R}_0(0)$

Note that the relationship between the indicators I_1 and I_2 may differ depending on the type of mechanism analyzed, the type of fault, and its stage of development.

3. Real vibration signal processing

A NELCON Port crane with a FLENDER D 46393 Bocholt gearbox driven by two identical Siemens 1LL8 317-4 PC-Z motors [20] was the subject of our investigation (Figure 1). The main parameters of a single motor were as follows: power – 400 kW, nominal rotational speed 1495 rpm, cosφ 0.88. Vibration signals were acquired simultaneously by two piezoceramic accelerometers fixed onto the cast iron body with powerful magnets, close to the cage of the bearing, on top of the motor. The sensitive axis of the sensors was set to the vertical direction to coincide with direction of gravity, to provide a maximum range for the vibration signal (in accordance with [21−25]). Data acquisition system settings were tuned to a filter cutoff frequency of 12.5 kHz with a sampling frequency of 25 kHz. The signals were stored on the hard disk of a notebook, and were processed offline with PNRP methods.

We consider the frequency band [0 Hz, 2 kHz]. The segment of the realization of signal is shown in Figure 1. To ascertain its covariance properties and spectral composition, we calculate the covariance function and spectral density for the stationary approximation, using the formulae:

$$\hat{R}(jh)=\frac{1}{2K+1}\sum_{n=-K}^{K}\left[\overset{\circ}{\xi}(nh)-\hat{m}\right]\left[\overset{\circ}{\xi}((n+j)h)-\hat{m}\right], \quad \hat{m}=\frac{1}{2K+1}\sum_{n=-K}^{K}\overset{\circ}{\xi}(nh) \tag{9}$$

$$\hat{f}(\omega)=\frac{h}{2\pi}\sum_{n=-L}^{L}k(nh)\hat{R}(nh)\cos\omega nh \qquad (10)$$

where $L=\dfrac{\tau_m}{h}$ is some natural number, τ_m is the of the correlogram cut-off and is $k(nh)$ the Hamming window:

$$k(\tau)=\begin{cases}0{,}54+0{,}46\cos\pi\tau/\tau_m, & |\tau|\le\tau_m,\\ 0, & |\tau|>\tau_m.\end{cases}$$
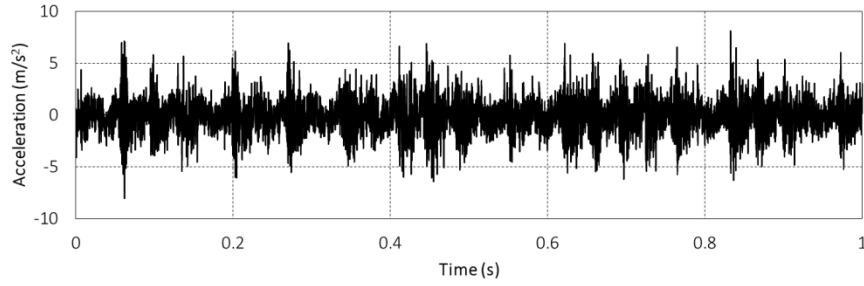

Figure 1. Segment of signal realization

Graphs of the estimators for the covariance function (9) and spectral density (10) are shown in Figure 2. The time-averaged power of the signal in the low-frequency band is $R(0)=1.23\,(m/s^2)^2$. The covariance function estimator has an undamped tail (Figure 5a) which can be explained by the presence of deterministic oscillations in the signal, with power of $0{,}3\,(m/s^2)$, equal to 0.25 of the signal power in this frequency range. The deterministic oscillations cause sharp peaks in the spectral density estimator (Figure 5b).
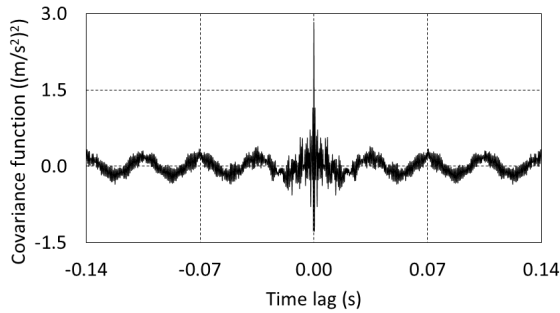
Figure 2. Estimator of covariance function
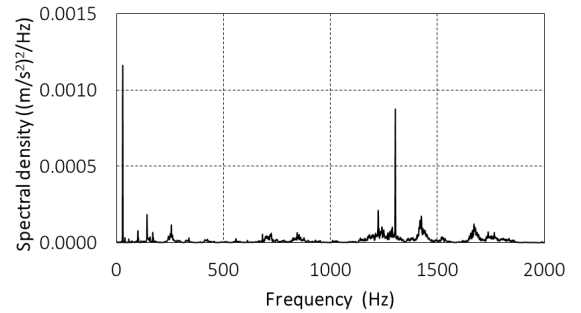
**Figure 3.** Estimator of spectral density

We separate the deterministic oscillations and compute their amplitude spectrum. To do this, we first use the functional in (1) to determine their basic frequency. The dependence of this functional on the test frequency is shown in Figure 3.

As we can see, the maximum value of this quantity is reached at $f=28.56\,Hz$, which we accept as the basic frequency estimator $\hat{f}_0$. By inserting this value into (2) $f=\hat{f}_0$, we can calculate the Fourier coefficients of the mean function and hence the amplitude spectrum (4). A diagram of the latter is shown in Figure 4b, and the numerical values of the harmonic amplitudes are listed in Table

1. As expected, the first harmonic has the largest amplitude, exceeding the second harmonic by more than nine times.

Table 1. Amplitudes of harmonics for deterministic oscillations

k	$A_k, \mathrm{m/s}^2$	k	$A_k, \mathrm{m/s}^2$	k	$A_k, \mathrm{m/s}^2$
0	0,000998	7	0,004026	14	0,005801
1	0,578998	8	0,013660	15	0,016205
2	0,063257	9	0,022912	16	0,014219
3	0,010482	10	0,020099	17	0,004295
4	0,029494	11	0,009993	18	0,028791
5	0,058225	12	0,038104	19	0,012165
6	0,058380	13	0,008142	20	0,018531
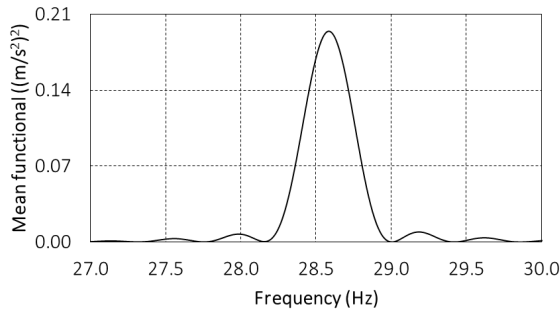
Figure 4. Dependence of functional (1) on test frequency
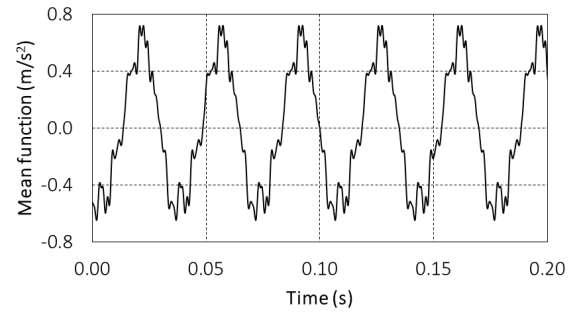

Figure 5. Estimator of mean function

The graph of the time dependence of the deterministic component obtained using the interpolation formula

$$\hat{m}(t) = \sum_{k=1}^{20} \left(\hat{m}_k^c \cos 2k\pi \hat{f}_0 t + \hat{m}_k^s \sin 2k\pi \hat{f}_0 t \right)$$

therefore has the form of a basic harmonic, on which the low-power oscillations of the harmonic with higher frequency are superposed (Figure 4a).

By separating the stochastic component $\overset{\circ}{\xi}(nh) = \xi(nh) - \hat{m}(nh, \hat{f}_o)$, we can identify the hidden periodicity of the second order. The dependence of the quadratic functional in (5) on the test frequency is shown in Figure 5. The clear, strong peak in the graph shows that the power of the stochastic part changes periodically over time. The maximum point of the functional in (5) is considered here as the estimator of the variance basic frequency $\hat{f}_0 = 28.43\,Hz$. The difference between this value and mean basic frequency obtained above is only $0.13\,Hz$, which can be considered the statistical error in the estimation.
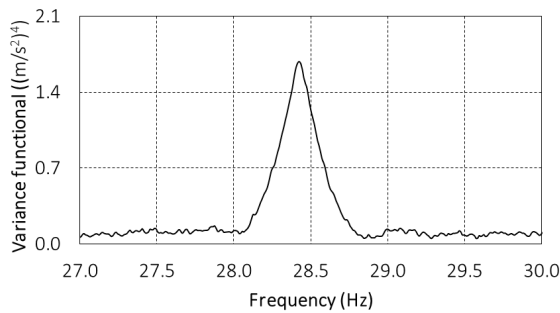
Figure 6. Dependence of functional (5) on test frequency
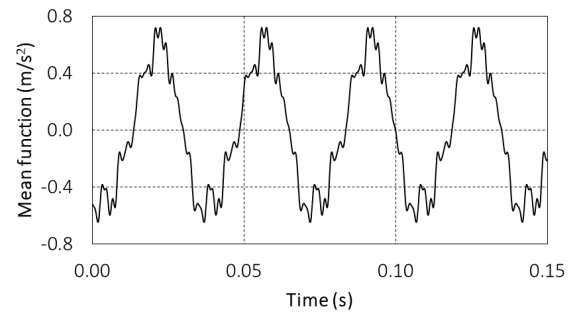
Figure 7. Estimator of variance

A diagram of the variance amplitude spectrum, calculated based on the relations in (6) and (8) for , $f=\hat{f}_0=28.43\,Hz$ is shown in Figure 6b, and the numerical values of the amplitudes are listed in Table 2.

Table 2. Amplitudes of variance harmonics.

k	$\hat{V}\left(k\hat{f}_0\right),\left(\text{m/s}^2\right)^2$	k	$\hat{V}\left(k\hat{f}_0\right),\left(\text{m/s}^2\right)^2$	k	$\hat{V}\left(k\hat{f}_0\right),\left(\text{m/s}^2\right)^2$
0	2,688626	7	0,069275	14	0,084981
1	1,487577	8	0,075994	15	0,109442
2	0,733531	9	0,108978	16	0,106775
3	0,343239	10	0,078820	17	0,056280
4	0,096395	11	0,092903	18	0,088458
5	0,269881	12	0,022760	19	0,031952
6	0,089720	13	0,029764	20	0,037484

It is evident that the variance amplitude spectrum is narrow, and the dominant part of the power for variance time changes belongs to the first five harmonics. The sum of the amplitudes for 20 harmonics is equal $4.014\left(m/s^2\right)^2$ to while the time-averaged value of the variance is equal to $R_0^I(0)=2.689\left(m/s^2\right)^2$. Thus, for the indicator of the periodical non-stationarity of the second order, we have $I_2^I=\sum\limits_{k=1}^{20}\hat{V}^I(k\,\hat{f}_0)/R_0^I=1.43$. A graph of the time dependence of the variance, which was calculated on the basis of the interpolation formula in (7), is presented in Figure 6a. In the same way as for the mean time changes, the oscillations at the basic frequency are most noticeable in this graph.

4. Conclusions

We have shown that the low-frequency component of the motor vibrations (< 2 kHz) is described by the PNRP model, where the basic frequency is determined by the shaft rotation frequency. The first harmonics of the amplitude spectra of the mean function and variance time changes are dominant, allowing us to deduce that these vibrations result from the rotor imbalance. This implies that the defect affects the properties of both the deterministic and stochastic parts of the vibration. The condition of the motor can therefore be characterized by the indicators of the first (I_1) and the second (I_2) orders.($_1$ is defined as the ratio of the total power of the harmonics of the deterministic oscillations to the time-averaged power of the stochastic part. I_2 is equal to the ratio of the sum of the amplitudes of the variance harmonics to its time-averaged value. It was found that in the case considered here, the numerical value of I_1 considerably exceeded the value of I_2. The values of the parameters describing the PNRP structure for the vibrations indicate that the motor's condition is unsatisfactory. Further research involves analyzing the high-frequency component of the vibration signal spectrum.

Declaration on Generative AI

The author(s) have not employed any Generative AI tools.

5. References

[1] Cyclostationarity in Communications and Signal Processing. Ed. by Gardner W.A. New York: IEEE Press, 1994.

[2] H. L. Hurd, A. Miamee. Perodically Correlated Random Sequences Spectral Theory and Practice. New Jersey: Wiley-Interscience, 2007.

[3] A. Napolitano. Cyclostationary Processes and Time Series: Theory, Applications, and Generalizations, Elsevier, Academic Press, 2020.

[4] R. Isermann. Fault-Diagnosis Applications. Model-Based Condition Monitoring: Actuators, Drives, Machinery, Plants, Sensors, and Fault-tolerant Systems. Springer-Verlag Berlin Heidelberg, 2011. doi: 10.1007/978-3-642-12767-0.

[5] J. Antoni. Cyclostationarity by examples. Mech. Syst. Signal Process. 23 (2009) 987–1036. doi: 10.1016/j.ymssp.2008.10.010

[6] C. Capdessus, M. Sidahmed, J. L. Lacoume. Cyclostationary Processes: Application in Gear Fault Early Diagnostics. Mech. Syst. Signal Process. 14 (2000) 371–385. doi: 10.1006/mssp.1999.1260.

[7] J. Antoni, F. Bonnardot, A. Raad, M. El Badaoui. Cyclostationary modeling of rotating machine vibration signals. Mech. Syst. Signal Process. 18 (2004) 253–265. doi: 10.1016/S0888-3270(03)00088-8.

[8] Z. K. Zhu, Z. H. Feng, K. Fanrang. Cyclostationary analysis for gearbox condition monitoring: Approaches and effectiveness. Mech. Syst. Signal Process. 19 (2005) 467–482. doi: 10.1016/j.ymssp.2004.02.007.

[9] A. E. Del Grosso. Structural Health Monitoring: research and practice. Second Conference on Smart Monitoring, Assessment and Rehabilitation of Civil Structures (SMAR 2013). URL: www.researchgate.net/publication/261119109.

[10] A. E. Del Grosso, F. Lanata. Reliability estimate of damage identification algorithms. Reliability Engineering and Risk Management, 2012, 350–355. URL: https://www.researchgate.net/publication/235329357.

[11] I. Javorskyj, P. Kurapov, R. Yuzefovych. Covariance characteristics of narrowband periodically non-stationary random signals. Mathematical Modeling and Computing 6 (2019) 276–288. doi: 10.23939/mmc2019.02.276

[12] I. Javorskyj, I. Matsko, R. Yuzefovych, Z. Zakrzewski. Discrete estimators of characteristics for periodically correlated time series. Digital Signal Processing 53 (2016) 25–40. doi: 10.1016/j.dsp.2016.03.003

[13] Y. Kharchenko, L. Dragun. Mathematical modeling of unsteady processesin electromechanical system of ring-ball mill. Diagnostyka. 18 (2017) 25–35. URL: http://www.diagnostyka.net.pl/pdf-68437-17747

[14] Engineering Dynamics and Vibrations: Recent Developments. Edited by Junbo Jia, Jeom Kee Paik. Editors, CRC Press, 2018. doi: 10.1201/9781315119908.

[15] G. W. Vogl, B. A. Weiss, M. A. Donmez. NISTIR 8012 Standards Related to Prognostics and Health Management (PHM) for Manufacturing: National Institute of Standards and Technology U.S. Department of Commerce. URL: https://tsapps.nist.gov/publication/get_pdf.cfm?pub_id=916376.

[16] P. D. McFadden, J. D. Smith. Vibration monitoring of rolling element bearings by the high frequency resonance technique – a review. Tribol. Int.17 (1984) 3–10. doi: 10.1016/0301-679X(84)90076-8.

[17] I. Javorskyj, R. Yuzefovych, P. Kurapov. Periodically non-stationary analytic signals and their properties // International Scientific and Technical Conference on Computer Sciences and Information Technologies, vol. 1, 7 November 2018, P. 191–194. doi: 10.1109/STC-CSIT.2018.8526752

[18] I. Javorskyj, R. Yuzefovych, O. Lychak, R. Slyepko, P. Semenov. Detection of distributed and localized faults in rotating machines using periodically non-stationary covariance analysis of vibrations. Meas. Sci. Technology 34 (2023) 065102. doi: 10.1088/1361-6501/acbc93.

[19] I. D. Ho, R. B. Randall. Optimization of bearing diagnostic techniques using simulated and actual bearing fault signals. Mech. Syst. Signal Process. 14 (2000) 763–788. doi: 10.1006/mssp.2000.1304

[20] Siements Simotics TN Serie N-compact Asynchronmotor Typ 1LL8. Dokumentbestellnummer: A5E03472650. Siemens AG 2016.

[21] ISO 10816–1:1995. Mechanical vibration. Evaluation of machine vibration by measurements on non-rotating parts. Part 1: General guidelines. International Standard.

[22] ISO 13373–1:2002. Condition monitoring and diagnostics of machines. Vibration condition monitoring. Part 1: General procedures.

[23] ISO 13373–2:2005. Condition monitoring and diagnostics of machines. Vibration condition monitoring. Part 2: Processing, analysis and presentation of vibration data.

[24] J. T. Broch, J. Courrech, J. Hassall at al. Mechanical Vibration and Shock Measurements. Bruel & Kjaer, 1984.

[25] R. Yuzefovych, I. Javorskyj, O. Lychak, R. Khmil, G. Trokhym. Analysis of the vibration signals based on PCRP representation. Ceur Workshop Proceedings. 4rd International Workshop on Information Technologies: Theoretical and Applied Problems (ITTAP-2024), Ternopil, Ukraine, 23-25 October 2024, 3896, P. 186–193. https://ceur-ws.org/Vol-3896/short5.pdf